https://doi.org/10.22226/2410-3535-2022-4-433-438

Electron-ion-plasma boriding of a multilayer nanostructural high-entropy alloy

Yu. F. Ivanov†, V. V. Shugurov, E. A. Petrikova, N. A. Prokopenko,

A. D. Teresov, O. S. Tolkachev

†yufi55@mail.ru

Institute of High Current Electronics SB RAS, Tomsk, 634055, Russia

The structure and properties of a high-entropy alloy (HEA) subjected to saturation with boron atoms by a combined electron-ion-plasma method are characterized. On a HEA film of 5 μm thickness deposited on AISI 304 steel, a film (boron + chromium) with a thickness of 1 μm was deposited and then the system "(Cr + B) film/(HEA film deposited on AISI 304 steel) substrate" was irradiated with a pulsed electron beam. It is shown that the wear resistance of the resulting alloy is more than 30 times higher than that of the original HEA film. The microhardness of the alloy is 10.5% higher than that of HEA in the initial state. It has been revealed that irradiation of the system with a pulsed electron beam leads to the formation of a multi-element surface alloy of composition (at.%) 5.8Al-11.6Ti-12.9Cr-13.0Fe-2.4Ni-13.1Cu-10.4Zr-8.8Nb, the rest (22 at.%) is oxygen and boron. Thus, seven-element HEA of non-stoichiometric composition, the concentration of metal elements of which varies within (5.8–13.0) at.%, and additionally containing atoms of nickel, oxygen and boron was formed. It has been established that the high tribological and strength properties of the surface alloy are due to the formation of a multiphase submicron-nanocrystalline structure of high-speed cellular crystallization in the modified layer 6 μm thick. High-speed crystallization is accompanied by alloy delamination with the formation of extended interlayers enriched with copper atoms located along the boundaries of crystallization cells.

Keywords: high-entropy alloy, boron, nanostructure, film/substrate system, pulsed electron beam, ion-plasma method.

1. Introduction

Diffusion saturation of the surface layer of metals and alloys with boron is one of the methods of chemical-thermal treatment aimed at hardening the surface of machine parts and mechanisms. Most often, surface borating is used to increase the wear resistance and hardness of parts and products when working in aggressive and abrasive media at high temperatures [1]. A common disadvantage of boriding methods used in industry is the duration of diffusion saturation and high process temperatures. To eliminate these disadvantages, the methods of intensifying this process are developed by using concentrated energy flows (laser beams [2–4], high frequency currents heating methods [5], pulsed and continuous electron beams [6–8], plasma flows [9–11], ion implantation [12], etc.). The last decades are characterized by active research of multielement alloys of equiatomic composition called high-entropy alloys (HEA) [13,14]. Numerous studies demonstrate the unique properties of these materials and predict their soon widespread use in various industries [15–18]. One of the options for improving the service characteristics of HEA is to saturate them with boron atoms. Various methods of HEA boriding are used: using nanosized borating powders [19,20], plasma borating [21], using laser technologies [22] and plasma spark sintering technologies [23], and many others.

The purpose of this work is to certify the structure and properties of a high-entropy alloy (25.7Ti-17.0Al-21.9Nb-22.3Zr-13.1Cu, at.%) subjected to electron-ion-plasma boriding.

2. Materials and experimental methods

Films of a high-entropy alloy of the Ti-Al-Cu-Zr-Nb composition with a thickness of 5 μm were used as the research material. HEA films were sputtered onto specimens (substrates) of AISI 304 steel and WC8 hard alloy. The formation of the HEA film was carried out on the QUINTA installation [24] by simultaneous ion-plasma sputtering of cathodes of copper, zirconium, niobium and Ti-50 at.% Al alloy. The method of forming HEA films is considered in detail in [25]. The HEA films were saturated with boron atoms in two stages. At the first stage, a film (boron + chromium) with a thickness of 1 μm was deposited on the HEA surface. The sputtering was carried out on the COMPLEX installation [26]. The basis of the system is a thermionic-cathode plasma source (PINK) and a DI80 arc evaporator [27]. A graphite crucible with boron powder was used as the PINK discharge anode. Due to the small size of the anode, the functioning of the non-self-sustained PINK gas discharge is difficult, resulting in a positive anode drop, which accelerates the plasma electrons to the anode.

This leads to intense heating of the anode. With increasing temperature, the conductivity of boron increases and the conductivity of graphite decreases. When the temperature reaches the order of (873 – 973) K, the discharge current switches to the surface of the boron powder, which leads to its intense heating and evaporation, i.e. formation of boron plasma. A diagram explaining the process of co-deposition of boron and chromium is shown in Fig. 1. Studies have shown that the time of deposition of films (Cr + B) with a thickness of 1 μm is 31.5 minutes. The temperature of the substrate during deposition was (723 – 773) K.

At the second stage, the "film (Cr + B)/(HEA) substrate" system formed in this way was irradiated with an intense pulsed electron beam for the purpose of liquid-phase mixing of the film and substrate elements. Irradiation of the "film (Cr + B)/(HEA) substrate" system was carried out with a pulsed electron beam using a SOLO installation [28] at the following electron beam parameters: 18 keV; (20, 30, 40) J/cm^2; 200 μs; 10 pls.; 0.3 s^{-1}. The working chamber was pumped to a pressure of $2 \cdot 10^{-3}$ Pa before irradiation, then argon was injected bringing the pressure in the working chamber to 0.02 Pa.

Investigations of the elemental and phase composition, defective substructure of the material were carried out by scanning (SEM 515 Philips with EDAX ECON IV microanalyzer) and transmission diffraction (JEM-2100F JEOL, the equipment of the CSU NMNT TPU) electron microscopy. Figure 2 shows a scheme of the study of a specimen subjected to boriding by SEM and TEM analysis. Mechanical properties were characterized by microhardness (PMT-3, indenter load was 0.5 N), tribological (TRIBOtester; Pin-On-Disc) — wear resistance and friction coefficient (counter-body — a ball (WC) with a diameter of 6 mm, wear track diameter was 4 mm with load of 2 N, friction path length of 100 m, specimen rotation speed of 25 mm/s (dry friction conditions at room temperature).

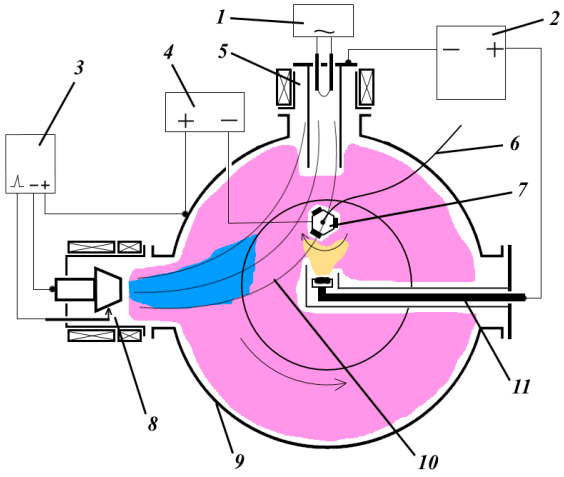

Fig. 1. (Color online) Scheme of film deposition (Cr + B). 1 — power supply unit for thermionic cathode of the PINK, 2 — power supply unit for the PINK discharge, 3 — power supply unit for the arc discharge evaporator of metal, 4 — electric bias power supply unit, 5 — PINK plasma generator, 6 — thermocouple, 7 — holder with specimens, 8 — arc discharge evaporator of chromium, 9 — vacuum chamber, 10 — magnetic field lines, 11 — heated anode input [25].

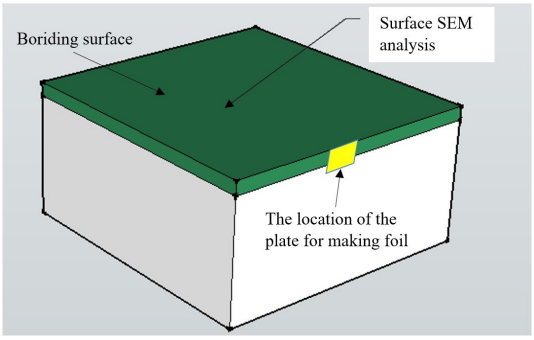

Fig. 2. (Color online) Scheme of the study of a specimen subjected to boriding by SEM and TEM analysis.

3. Results and discussion

Scanning electron microscopy methods have shown that an inhomogeneous structure is formed on the specimen surface as a result of irradiation (Fig. 3). It can be assumed that the high-speed thermal action of the pulsed electron beam led to partial melting of the "film (Cr + B)/(HEA) substrate" system. Subsequent high-speed crystallization is accompanied by the formation of an islet-type structure, in which islets of light contrast are bordered by extended layers of dark contrast (Fig. 3 a, c, d). Islets and interlayers separating them contain inclusions of a rounded or globular shape. The size of inclusions in the islets and interlayers separating them depend on the energy density of the electron beam and vary over a wide range.

Considering the results of determining the microhardness and wear resistance, further structural-phase studies were carried out for the specimen obtained by irradiating the "(Cr + B) film/(HEA) substrate" system with a pulsed electron beam with an electron beam energy density of 30 J/cm^2. Using X-ray microanalysis methods, it was shown that irradiation of the "film (Cr + B)/(HEA) substrate" system with a pulsed electron beam leads to the formation of a multi-element surface layer of the (at.%) 5.8Al-11.6Ti-12.9Cr-13.0Fe-2.4N-13.1Cu-10.4Zr-8.8Nb composition, the rest (22 at.%) oxygen + boron. Thus, an alloy is formed, the concentration of metallic elements of what (excluding Ni) varies within (5.8 –13.0) at.%, i.e. a seven-element HEA of non-stoichiometric composition is formed, additionally containing oxygen and boron atoms.

A non-uniform distribution of chemical elements in the surface layer of the investigated alloy (Fig. 4) was revealed by the mapping method. It has been established that islands of light contrast are enriched mainly in atoms that form the initial HEA; the interlayers separating them are enriched mainly in chromium, boron, and oxygen atoms.

The results of studying the defective substructure of the "film (Cr + B)/(HEA) substrate" system irradiated with a pulsed electron beam, obtained by transmission electron microscopy, are shown in Figs. 5 and 6. It can be stated that in the surface layer with $a \approx 6$ μm thickness (Fig. 5) a submicron-nanocrystal structure is formed.

A transition layer is observed at a distance of ≈8 μm from the irradiation surface, what has the high-speed crystallization structure of the substrate (AISI 304 steel) (Fig. 6 a), there is a polycrystalline structure of steel (Fig. 6 b) at a distance of 10 μm or more.

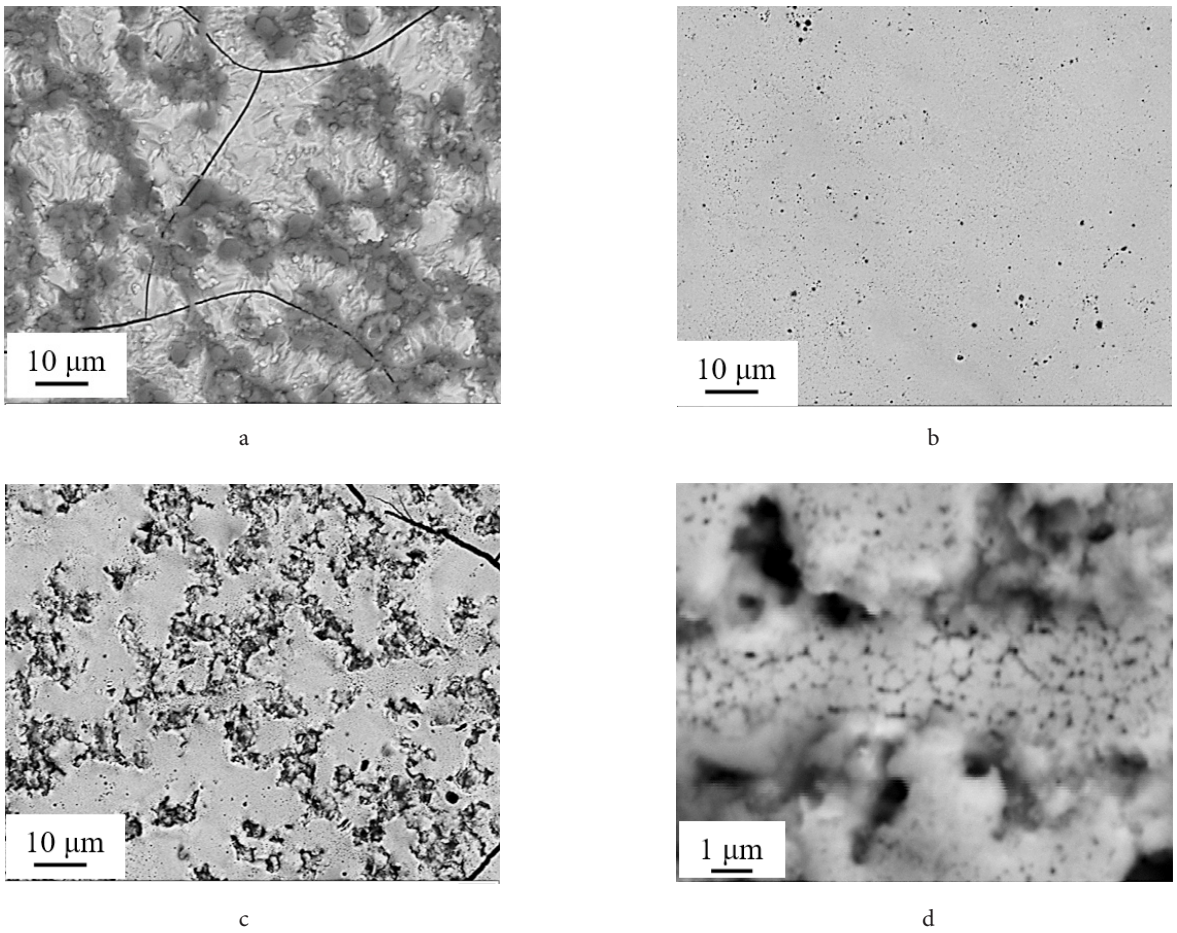

Fig. 3. Electron microscopic images of the surface structure of the HEA specimen modified by irradiating the "film (Cr + B)/(HEA) substrate" system with a pulsed electron beam of energy density (J/cm^2) of 20 (a), 40 (b), 30 (c, d).

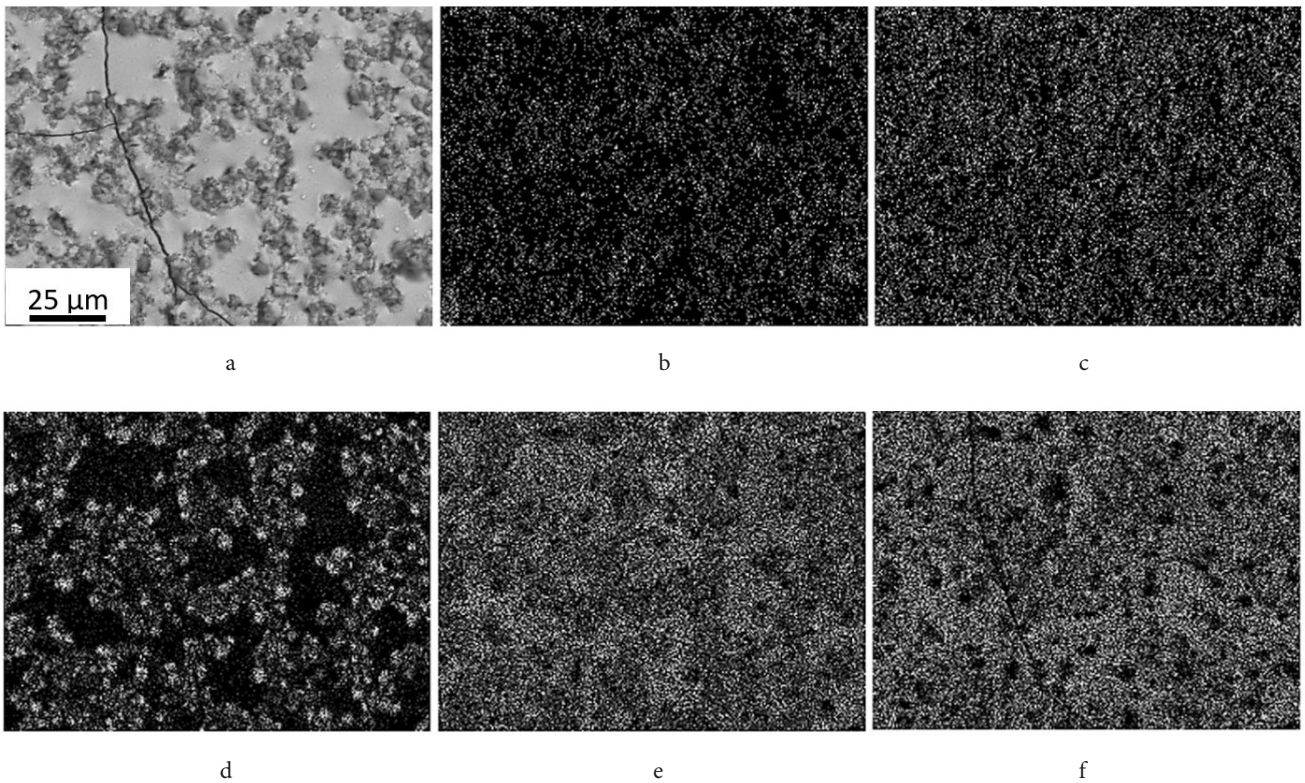

Fig. 4. Electron microscopic images of the HEA specimen surface structure modified by irradiating the "film (Cr + B)/(HEA) substrate" system with a pulsed electron beam with an electron beam energy density of 30 J/cm^2 (a); images of this area of the specimen obtained in the characteristic X-ray radiation of boron (b), oxygen (c), chromium (d), copper (e), and niobium (f) atoms.

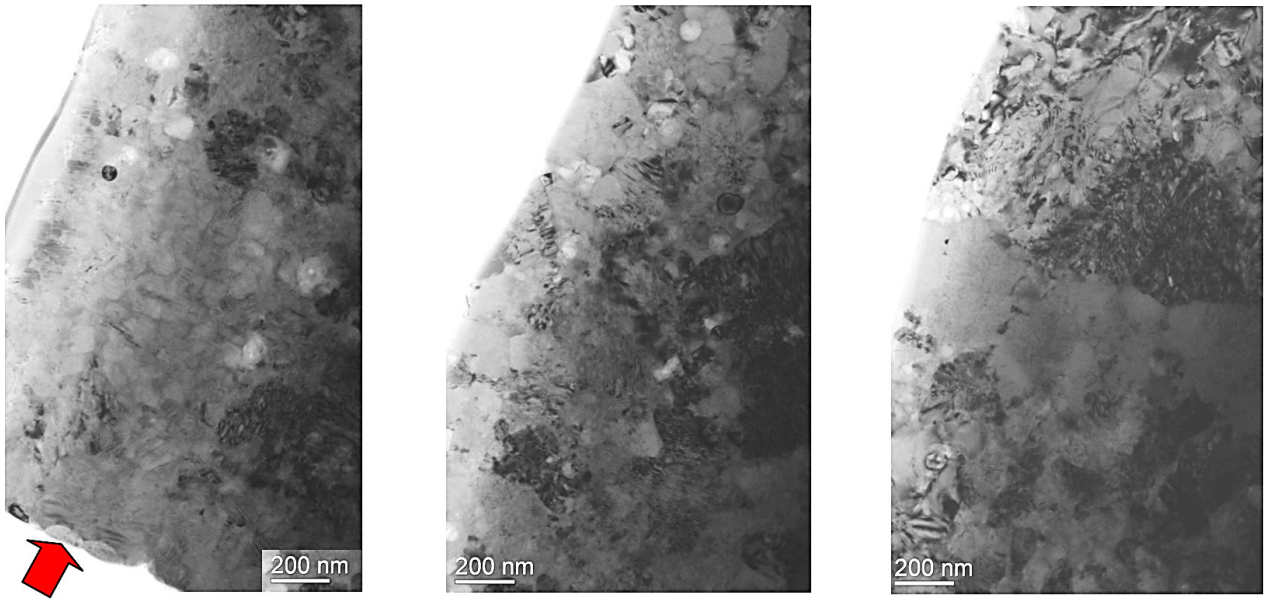

a b c

Fig. 5. Electron microscopic image of the HEA specimen structure modified by irradiating the "(Cr + B) film/(HEA) substrate" system with a pulsed electron beam with an electron beam energy density of 30 J/cm^2; layer adjacent to the specimen surface (a), located at a distance of 2 μm (b), and 6 μm from the irradiation surface (c); the arrow indicates the irradiation surface.

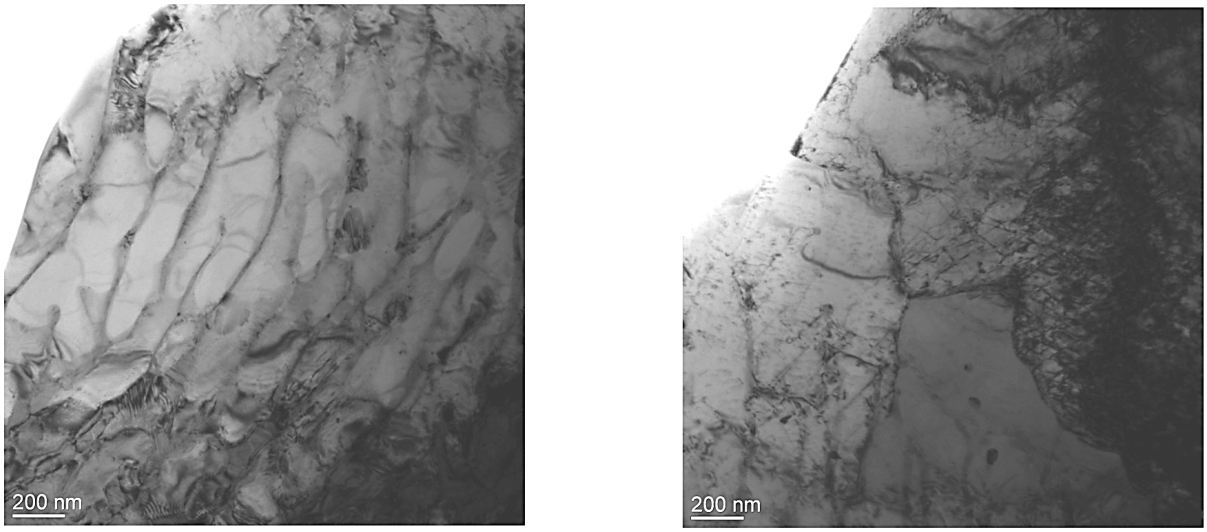

a b

Fig. 6. Electron microscopic image of the of AISI 304 steel structure (substrate) modified as a result of irradiation of the "film (Cr + B)/(HEA) substrate" system with a pulsed electron beam; layer located at a distance of 8 μm (a), 10 μm (b).

The distribution of chemical elements in the surface layer of the "film (Cr + B)/(HEA) substrate" system irradiated with a pulsed electron beam was studied using X-ray microanalysis methods. The separation of the alloy with the formation of extended interlayers enriched with copper atoms, located along the boundaries of the high-speed crystallization cells, was revealed (Fig. 7).

Summarizing the results of studying of the surface layer structure "(Cr + B) film/(HEA) substrate" system with a pulsed electron beam with an electron beam energy density of 30 J/cm^2, in Fig. 8 is a diagram of the layer-by-layer of structural elements arrangement, the electron microscopic image of what is shown in Figs. 3 – 7.

It was shown in [25] that the microhardness of the HEA film is 11.3 GPa, the wear parameter (the reciprocal of wear resistance) is $2.2 \cdot 10^{-4}$ mm^3/N · m, and the friction coefficient is 0.79. The formation of the "film (Cr + B)/(HEA) substrate" system and its subsequent irradiation with a pulsed electron beam leads to a significant increase in the wear resistance of the material. Namely, the wear parameter, regardless of the energy density of the electron beam, decreased to $(0.5 – 0.7) \cdot 10^{-5}$ mm^3/N · m, friction coefficient — up to 0.61, i.e. more than 30 and 1.3 times relative to the original HEA film. The microhardness depends more significantly on the energy density of the electron beam and reaches its highest value, equal to 12.4 GPa, when the "film (Cr + B)/(HEA) substrate" system is irradiated with a pulsed electron beam with an energy density of 30 J/cm^2, i.e. exceeds the microhardness of the original film on 10.5%. Obviously, the relatively high tribological properties of the formed surface

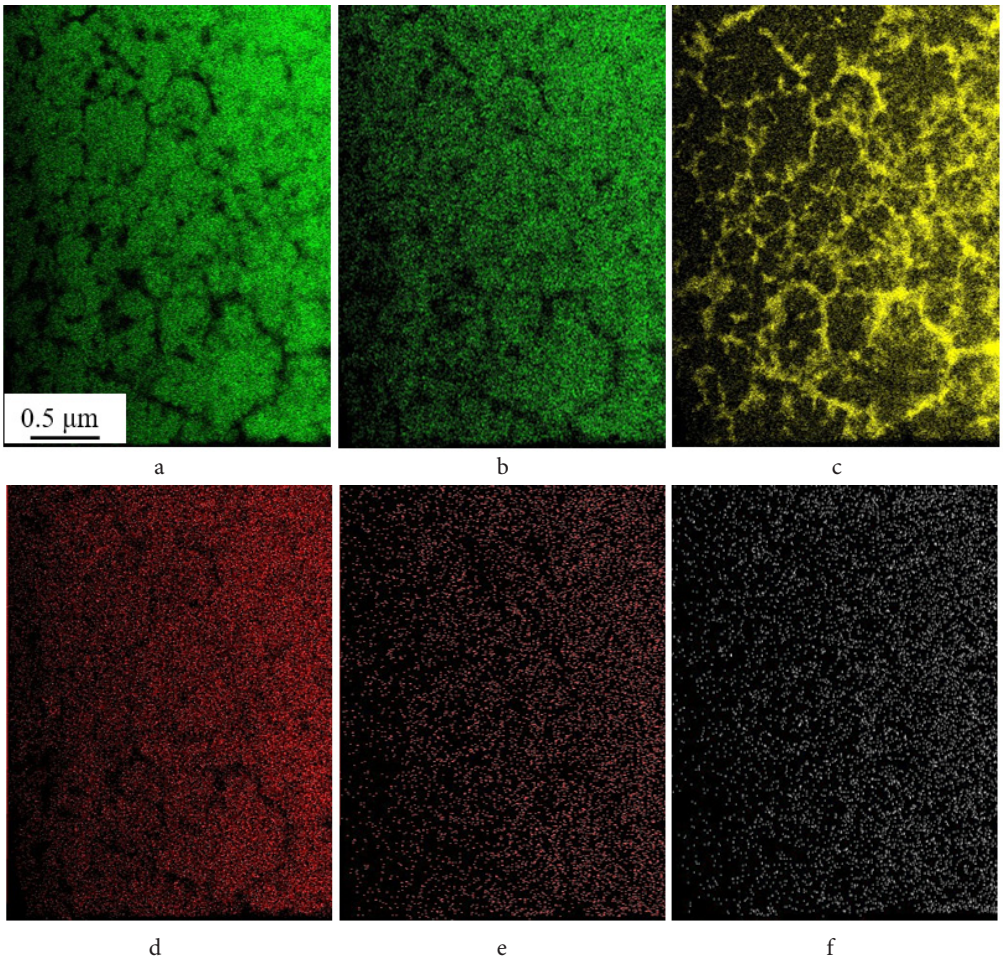

Fig. 7. (Color online) Images of the HEA specimen structure modified by irradiating the "(Cr + B) film/(HEA) substrate" system with a pulsed electron beam with an electron beam energy density of 30 J/cm^2, obtained in the characteristic X-ray radiation of iron atoms (a), chromium (b), copper (c), titanium (d), niobium (e), zirconium (e).

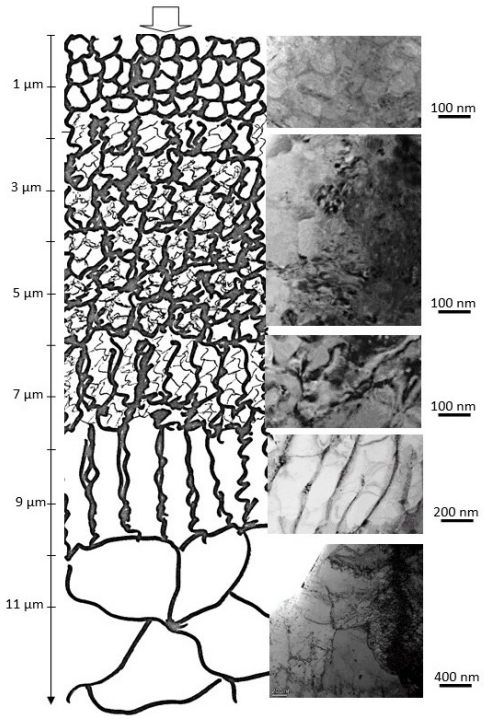

Fig. 8. Schematic representation of the surface layer structure "(Cr + B) film/(HEA) substrate" system with a pulsed electron beam with an electron beam energy density of 30 J/cm^2; the arrow indicates the irradiation surface.

alloy are due to the formation of a multilayer multiphase multielement submicro-nanocrystalline structure of high-speed cellular crystallization.

4. Conclusions

A multi-element surface alloy with a ≈6 μm thickness of the 5.8Al-11.6Ti-12.9Cr-13.0Fe-2.4Ni-13.1Cu-10.4Zr-8.8Nb, the rest (22 at.%) is oxygen + boron composition (at.%) was created by complex electron-ion-plasma method, combining the formation of the "film (Cr + B)/(HEA film deposited on AISI 304 steel) substrate" system and subsequent pulsed electron beam treatment. It was shown that the wear parameter (the reciprocal of wear resistance) of the resulting alloy is more than 30 times less than the wear parameter of the original HEA film. The microhardness of the formed alloy is 10.5% higher than the microhardness of the HEA in the initial state. It has been established that the high tribological properties of the surface alloy are due to the formation of a multi-element submicron-nanocrystalline structure of high-speed cellular crystallization. It is shown that the crystallization of the surface alloy is accompanied by material stratification with the formation of extended interlayers enriched with copper atoms located along the boundaries of high-speed crystallization cells.

Acknowledgements. The study was supported by the Russian Science Foundation grant № 19-19-00183, https://rscf.ru/project/19-19-00183/.

References

1. L. G. Voroshnin, A. A. Aliev. Boriding from pastes. Astrakhan, ASTU (2006) 287 p. (in Russian)
2. S. Sashank, P. D. Babu, P. Marimuthu. Surface & Coatings Technology. 363, 255 (2019). Crossref
3. D. Mikołajczak, M. Kulka, N. Makuch, P. Dziarski. Arch Mech Tech Mater. 36, 35 (2016). Crossref
4. P. Kieruj, N. Makuch, M. Kukliński. MATEC Web of Conferences. 188, 02003 (2018). Crossref
5. S. Dmitriev, V. Malikov, A. Sagalakov, A. Grigorev, A. Ishkov. Advances in Engineering Research. 158, 88 (2018).
6. A. A. Novakova, I. G. Sizov, D. S. Golubok, T. Y. Kiseleval, P. O. Revokatov. J Alloy Compd. 383, 108 (2004). Crossref
7. I. A. Bataev, A. A. Bataev, M. G. Golkovski, D. S. Krivizhenko, A. A. Losinskaya, O. G. Lenivtseva. Appl. Surf. Sci. 284, 472 (2013). Crossref
8. B. D. Lygdenov, V. A. Butukhanov, J. Ying. Modern science-intensive technologies. Region Application. 4 (44), 189 (2015).
9. P. N. Belkin, S. A. Kusmanov. Electronic processing of materials. 54 (5), 1 (2018). Crossref
10. O. A. Gómez-Vargas, J. Solis-Romero, U. Figueroa-López, M. Ortiz-Domínguez. Mater Lett. 176, 261 (2016). Crossref
11. P. N. Belkin, A. L. Yerokhin, S. A. Kusmanov. Surf Coat Technol. 307, 1194 (2016). Crossref
12. A. Singh, E. J. Knystautas. Appl Phys A. 40, 91 (1986). Crossref
13. B. Cantor, I. T. H. Chang, P. Knight, A. J. B. Vincent. Mater. Sci. Eng. A. 375 – 377, 213 (2004). Crossref
14. E. J. Pickering, N. G. Jones. International Materials Reviews. 61, 183 (2016). Crossref
15. Y. F. Ye, Q. Wang, J. Lu, C. T. Liu, Y. Yang. Materials Today. 19, 349 (2016). Crossref
16. V. E. Gromov, S. V. Konovalov, Yu. F. Ivanov, K. A. Osintsev. Structure and properties of high-entropy alloys. Springer Nature, Switzerland, Advanced Structured Materials (2021) 107 p. Crossref
17. D. B. Miracle, O. N. Senkov. Acta Materialia. 122, 448 (2017). Crossref
18. S. Praveen, H. S. Kim. Adv. Eng. Mater. 20, 1 (2018). Crossref
19. A. Günen. Surface & Coatings Technology. 421, 127426 (2021). Crossref
20. A. Erdogan, A. Günen, M. S. Gok, S. Zeytin. Vacuum. 183, 109820 (2021). Crossref
21. B. Storr, L. Moore, K. Chakrabarty, Z. Mohammed, V. Rangari, C.-C. Chen, S. A. Catledge. APL Mater. 10, 061109 (2022). Crossref
22. D. Liu, J. Zhao, Y. Li, W. Zhu, L. Lin. Appl. Sci. 10, 49 (2020). Crossref
23. H. Nakajo, A. Nishimoto. J. Manuf. Mater. Process. 6, 29 (2022). Crossref
24. N. N. Koval, Yu. F. Ivanov, V. N. Devyatkov, V. V. Shugurov, A. D. Teresov, E. A. Petrikova. Izvestija VUZov Fizika. 63, 174 (2020). (in Russian) Crossref
25. N. A. Prokopenko, E. A. Petrikova, V. V. Shugurov, M. S. Petykevith, Yu. F. Ivanov, V. V. Uglov. IOP Conf. Series: Materials Science and Engineering. 1093, 012025 (2021). Crossref
26. V. Devyatkov, Yu. Ivanov, O. Krysina, N. Koval, E. Petrikova, V. Shugurov. Vacuum. 143, 464 (2017). Crossref
27. O. Krysina, N. Koval, I. Lopatin, V. Shugurov. Izvestija VUZov Fizika. 57 (11/3), 88 (2014). (in Russian)
28. Yu. F. Ivanov, O. V. Krysina, E. A. Petrikova, A. D. Teresov, V. V. Shugurov, O. S. Tolkachev. High Temperature Material Processes. 21 (1), 53 (2017). Crossref